Multirate Adaptive Robust Control with Position-dependent Nonlinearity for Tilting-table of Machine Tool: A Basic Study on Test-bench

葛　晨宇*，阮　平明，藤本　博志（東京大学）
寺田　祐貴，阪本　将隆（DMG 森精機株式会社）

Chenyu GE*, Binh-Minh NGUYEN, Hiroshi FUJIMOTO (The University of Tokyo)
Yuki TERADA, Masataka SAKAMOTO (DMG MORI CO.,LTD)

This paper presents an adaptive multirate control system that improves the tracking performance of the tilting part of the five-axis machine tools. To deal with the position-dependent nonlinearity, the multirate perfect tracking controller (PTC) is designed. The PTC is adaptively updated in real-time by a conditional recursive least-square(RLS) parameter identification algorithm.

Keywords: Machine Tool, Position-dependent Nonlinearity, Multirate Control, Parameter Identification

1. Introduction

Machine tool plays an irreplaceable role in manufacture. One of the most advanced type of machine tools, as shown in Fig. 1, is the five-axis machine. Such machines have 5 Degree-of-Freedoms (DoFs), which consists 3 DoFs of translation and 2 DoFs of rotation.

Considering the advanced tool machines, the position accuracy is of the most essential requirement. The control method that is most commonly used, also the easiest to apply, is the derivative controller [2] that includes the well-known proportional–integral–derivative controller (PID) [3] and the pseudo derivative feedback controller (PDF) [4]. The aforementioned feedback controllers can ensure the system stability, however, to improve the tracking performance and against the model uncertainty and nonlinearity, a feedforward controller is necessary. The model-based feedforward controllers have been proposed (5), (6). However, good performance of such controllers were achieved only when we can precisely know the system model, including the nonlinearity. To overcome such problems, adaptive feedforward control with compensation against nonlinearity was proposed [8]. However, this study does not consider the multi-sampling times, which is a real practical issue in the tool machine control. Besides, data-driven learning [7] [9] controllers are under developing that can reduce the dynamics modeling effort. However, this method require offline tuning process, which increases the burden to design and implement the controller in practical applications.

Fig.1　The overview of five-axis machine tool: 3 DoFs of translation(X-Y-Z) and 2 DoFs of rotation(A-C) [1]

With respect to the above discussion, this paper proposes a multirate position control system with the two degree of freedom configuration. This paper is motivated by the work of Fujimoto et al. on multirate robust adaptive control in 2005 [10]. The proposed system consists of a PID feedback controller and an adaptive feedforward controller which can compensate the nonlinearity.

The focus of this paper is position control of the rotating A-axis in Fig. 1. To this end, a testbench was build to imitate the movement of the tilting table. The test bench's nonlinear dynamics and parameter uncertainty are the most challenge, since they might deteriorate the performance of the feedback controller. To deal with this issue, the contribution of this paper can be considered as follows:

- Firstly, we modeled and built an unbalanced torque motor bench to simulate the tilting table.
- Secondly, a conditional recursive least-square(RLS) algorithm is established to identify not only the inertia and damping term but also the unbalance torque which associates with the nonlinearity.
- Last but not least, the identified parameters are used to update the multirate perfect tracking controller(PTC) and the multirate nonlinearity compensator in real-time.

2. System Modeling

〈2・1〉 Dynamics Modeling　To study the motion of the

tilting table in Fig. 1, this paper utilizes a 2-inertia motor bench as shown in Fig. 2. The load is assumed to be an uniform semi-circular disc, which generates an extra torque lead by gravity during the rotation of the system.

In the experimental setting of this study, the centre of gravity G is not in the geometric centre. Consequently, the torque generated by gravity F, marked as T_F, is relative to the position and their relation is given as:

$$T_F = Fd = FR\sin(\theta) \tag{1}$$

where R is the distance from the centre of gravity to the rotation axis, d is the magnitude of the position, m is the mass of the load and g represents the acceleration of gravity. Here, we define the maximum unbalanced torque $U = FR$. We give the dynamics formulation of the unbalanced torque based on a 2-inertia motor bench as:

$$\underbrace{J\ddot{\theta} + D\dot{\theta}}_{\text{Linear Dynamics}} + \underbrace{U\sin(\theta)}_{\text{Nonlinear Dynamics}} = T_m \tag{2}$$

where the system parameters J is the inertia [kg m^2], D is the damping [N m/(rad/s)].

〈2•2〉 State-space Modeling For the system described in equation (3), the state space of the model is given below, where the state variable are determined as $\boldsymbol{x} = \begin{bmatrix}\theta & \dot{\theta}\end{bmatrix}^{\mathrm{T}}$ where y is the position and $\dot{y}$ is the time differentiation of y and u is the input torque T_m:

$$\begin{aligned}\dot{\boldsymbol{x}} &= \boldsymbol{A}_c\boldsymbol{x} + \boldsymbol{B}_c(u - T_F) = \begin{bmatrix}0 & 1\\ 0 & -\frac{D}{J}\end{bmatrix}\boldsymbol{x} + \begin{bmatrix}0\\ \frac{1}{J}\end{bmatrix}u - \begin{bmatrix}0\\ \frac{1}{J}\end{bmatrix}T_F\\ y &= \boldsymbol{C}_c\boldsymbol{x} = \begin{bmatrix}1 & 0\end{bmatrix}\boldsymbol{x}\end{aligned} \tag{3}$$

The continuous time state-space needed to be discretized to design the feedforward controller and this would be introduced in the next section.

3. Control System Design

〈3•1〉 Proposed Methods The proposed control configuration is shown in Fig. 3 and Table 1, including the RLS parameter identification, the perfect tracking controller and the PID feedback controller. In addition, a multirate nonlinear compensator (MNC) is designed to deal with the position dependent nonlinearity and improve the control performance.

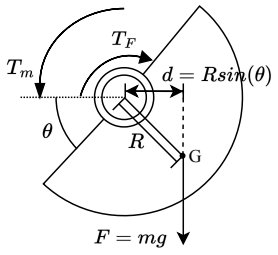

Fig.2 An illustration on the experimental test bench

Table 1 Overview of the proposed methods

Proposed Algorithm	Feedforward		Feedback
	Model for PTC	MNC	PID
I	Linear part of the system dynamics (see (3))	Compensation using the dynamics of the nonlinear part (see (13))	Section 4.1
II	Linearized state space (see (17))	Compensation by linearization (see (17))	

〈3•2〉 Conditional RLS RLS is an online parameter estimation tool [11] [10] calculates the system parameters $\boldsymbol{\vartheta} = \begin{bmatrix}J & D & U\end{bmatrix}^{\mathrm{T}}$, from the system input(s) u, and the system output(s) $\boldsymbol{\varphi} = \begin{bmatrix}\ddot{y} & \dot{y} & \mathrm{siny}\end{bmatrix}^{\mathrm{T}}$ using the equation below.

$$u = \boldsymbol{\varphi}^T\boldsymbol{\vartheta} = \begin{bmatrix}\ddot{y} & \dot{y} & \mathrm{siny}\end{bmatrix}\begin{bmatrix}J & D & U\end{bmatrix}^{\mathrm{T}} \tag{4}$$

The discrete-time RLS algorithm is expressed in (5). Notice that $\boldsymbol{\vartheta}$, $\boldsymbol{L}$ and $\boldsymbol{P}$ are updated only if the PE condition stated in (18) is satisfied. Otherwise, $\boldsymbol{\vartheta}[k] = \boldsymbol{\vartheta}[k-1]$, $\boldsymbol{L}[k] = \boldsymbol{L}[k-1]$ and $\boldsymbol{P}[k] = \boldsymbol{P}[k-1]$.

$$\hat{\boldsymbol{\vartheta}}[k] = \hat{\boldsymbol{\vartheta}}[k-1] + \mathrm{Proj}_{\hat{\boldsymbol{\vartheta}}}\{\boldsymbol{L}[k](u[k] - \boldsymbol{\varphi}^{\mathrm{T}}[k]\hat{\boldsymbol{\vartheta}}[k-1])\} \tag{5}$$

where covariance matrices $\boldsymbol{L}$ and $\boldsymbol{P}$ are updated following (6):

$$\begin{aligned}\boldsymbol{L}[k] &= \frac{\boldsymbol{P}[k-1]\boldsymbol{\varphi}[k]}{\lambda + \boldsymbol{\varphi}^{\mathrm{T}}[k]\boldsymbol{P}[k-1]\boldsymbol{\varphi}[k]}\\ \boldsymbol{P}[k] &= \frac{(\boldsymbol{I} - \boldsymbol{L}[k]\boldsymbol{\varphi}^{\mathrm{T}}[k])\boldsymbol{P}[k-1]}{\lambda}\end{aligned} \tag{6}$$

where λ is a forgetting factor which is slightly close to 1. Its value is selected via a fine-tuning process for good identification performance. The projection algorithm which guarantees that the estimated parameters do not break the designated limits, are given as below:

$$\mathrm{Proj}_{\hat{\boldsymbol{\vartheta}}_j}(\bullet_j) = \begin{cases}0, & \text{if } \hat{\boldsymbol{\vartheta}}_j \geq \boldsymbol{\vartheta}_{j_{max}} \text{ and } \bullet_j \geq 0\\ 0, & \text{if } \hat{\boldsymbol{\vartheta}}_j \leq \boldsymbol{\vartheta}_{j_{min}} \text{ and } \bullet_j \leq 0\\ \bullet_j, & \text{Otherwise.}\end{cases} \tag{7}$$

There are several practical way to verify the PE condition proposed in (10), (11) and (12). The persistent excitation condition can be verified through calculating the PE matrix $\boldsymbol{M}[k]$ expressed in (8).

$$\boldsymbol{M}[k] = \frac{1}{W}\sum_{l=k-W}^{k}\boldsymbol{\varphi}[l]\boldsymbol{\varphi}^{\mathrm{T}}[l] \tag{8}$$

In this study, the PE condition is verified by using the moving window with the length $W = 100$. We only need to examine the minimum eigenvalue of matrix $\boldsymbol{M}[k]$, defined as $\kappa[k]$, and PE condition is satisfied when $\kappa[k] > 0$. We show the PE index with our desired trajectory in Fig. 6.

〈3•3〉 Adaptive Perfect Tracking Controller There are

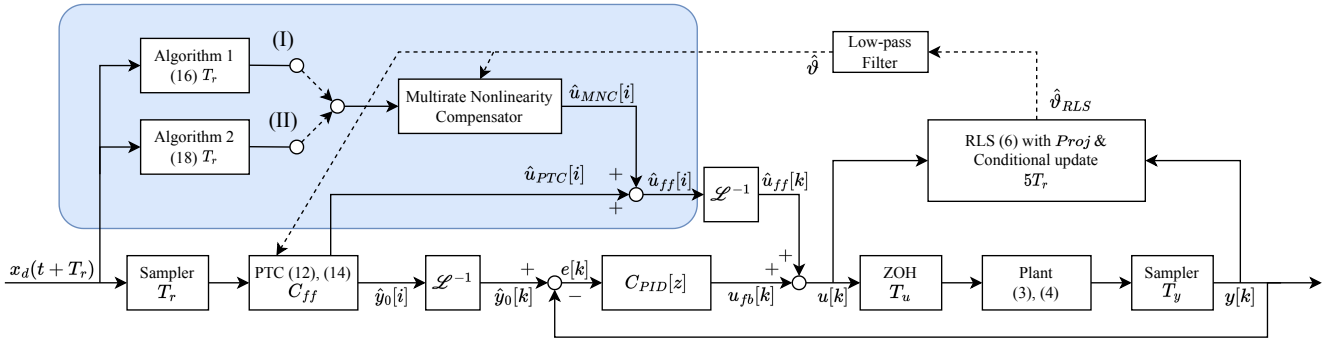

Fig.3 The proposed configuration of the multirate adaptive robust control system and the main contribution is highlighted. The discrete variables of $[i]$ are in the sample of T_r and those variables of $[k]$ are in the sample of T_y or T_u

2 sampling rates exist within the digital control system, T_r refers to the sampling rate of the desired trajectory, T_u refers to the sampling rate of the feedforward signal and T_y refers to the sampling rate of the encoder. The illustration of these sampling rates are shown in Fig. 4, where in this paper $T_r = 2T_y = 2T_u$ and θ_d denotes the desired trajectory in position.

〈3•3•1〉 Formulation of PTC The multirate PTC is designed based on the discretized linear part of (3) following the multirate PTC theory [6] [10].

$$\begin{aligned} \boldsymbol{x}[k+1] =& \boldsymbol{A}_d\boldsymbol{x}[k] + \boldsymbol{B}_d u[k] \\ y[k] =& \boldsymbol{C}_d\boldsymbol{x}[k] \end{aligned} \tag{9}$$

$$\boldsymbol{A}_d = e^{\boldsymbol{A}_c T_y}, \quad \boldsymbol{B}_d = \int_0^{T_y} e^{\boldsymbol{A}_c\tau}\boldsymbol{B}_c d\tau, \quad \boldsymbol{C}_d = \boldsymbol{C}_c$$

For the nonadaptive PTC, the multirate plant is given as:

$$\begin{aligned} \boldsymbol{x}_d[i+1] =& \boldsymbol{A}\boldsymbol{x}_d[i] + \boldsymbol{B}\boldsymbol{u}_{PTC}[i] \\ \boldsymbol{y}_0[i] =& \boldsymbol{C}\boldsymbol{x}_d[i] + \boldsymbol{D}\boldsymbol{u}_{PTC}[i] \end{aligned}$$

$$\left[\begin{array}{c|c} \boldsymbol{A} & \boldsymbol{B} \\ \hline \boldsymbol{C} & \boldsymbol{D} \end{array}\right] = \left[\begin{array}{c|cc} \boldsymbol{A}_d^2 & \boldsymbol{A}_d\boldsymbol{B}_d & \boldsymbol{B}_d \\ \hline \boldsymbol{C}_d & 0 & 0 \\ \boldsymbol{C}_d\boldsymbol{A}_d & \boldsymbol{C}_d\boldsymbol{B}_d & 0 \end{array}\right] \tag{10}$$

where the state variable $\boldsymbol{x}_d[i]$ is the desired reference $\boldsymbol{x}_d(t)$ sampled by the rate of T_r, the system nominal input $\boldsymbol{u}[i]$ are given as:

$$\begin{aligned} \boldsymbol{u}_{PTC}[i] &= \left[\boldsymbol{u}_{PTC}[k] \quad \boldsymbol{u}_{PTC}[k+1]\right]^{\mathrm{T}} \\ &= \boldsymbol{B}^{-1}(\boldsymbol{x}_d[i+1] - \boldsymbol{A}\boldsymbol{x}_d[i]) \end{aligned} \tag{11}$$

The discrete-time lifting operator $\mathscr{L}^{-1}$ in Fig. 3 is to transform the 2-dimension discrete-signal in a rate of T_r to a 2-serial discrete-signal in the rate of T_u.

〈3•3•2〉 Adaptive PTC The adaptive PTC will use the estimation of system parameters ϑ from the RLS, which is $\hat{\vartheta}$, to update the multirate state-space matrices in (10) and mark them as $\hat{\boldsymbol{A}}$, $\hat{\boldsymbol{B}}$, $\hat{\boldsymbol{C}}$, $\hat{\boldsymbol{D}}$. The feedforward command of adaptive PTC is:

$$\hat{\boldsymbol{u}}_{PTC}[i] = \hat{\boldsymbol{B}}^{-1}(\boldsymbol{x}_d[i+1] - \hat{\boldsymbol{A}}\boldsymbol{x}_d[i]) \tag{12}$$

〈3•4〉 Multirate Nonlinearity Compensator To deal with the nonlinearity, two multirate algorithms for nonlinear compensation are presented in this subsection.

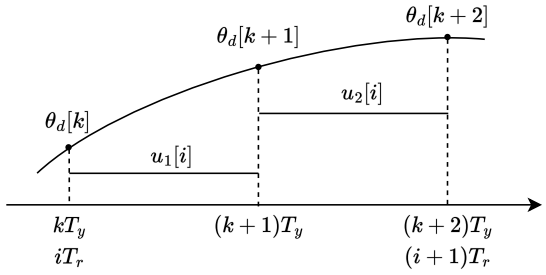

Fig.4 The schematic of the multirate system [10]

〈3•4•1〉 Adaptive PTC with Compensation of $U\sin\theta$ (Algorithm I) The most easy-coming-up method is to compensate the feedforward signal using the pre-calculated desired extra torque, which is the $U\sin\theta$ in (2). In this method, the PTC is designed base on the linear part of (3), (9) and (10). Besides, the MNC is shown in Fig. 3 joint (I), and the output of nonadaptive MNC is expressed as:

$$\boldsymbol{u}_{MNC}[i] = \left[U\sin(\theta_d[k]) \quad U\sin(\theta_d[k+2])\right]^{\mathrm{T}} \tag{13}$$

For the adaptive case, the U in (13) can be replaced by $\hat{U}$ from the RLS identification.

〈3•5〉 Model Decomposition (Algorithm II) Another idea is to decompose the system dynamics around the operating position $\theta_{offset}[i]$ of this control period from iT_r to $(i+1)T_r$. The operating position $\theta_{offset}[i]$ is defined as the desired start position in this period, which is a constant shown as $\theta_d[k]$ in Fig. 5. Base on the desired trajectory, the model is decomposed following $\theta = \theta_{offset} + \delta\theta$ as:

$$\begin{aligned} T_m &= J\delta\ddot{\theta} + D\delta\dot{\theta} + U\sin(\theta_{offset} + \delta\theta) \\ &= J\delta\ddot{\theta} + D\delta\dot{\theta} + U\sin\theta_{offset}\cos\delta\theta + U\cos\theta_{offset}\sin\delta\theta \end{aligned} \tag{14}$$

As we stated before, θ_{offset} is a constant with in a control period. Therefore, $\frac{d}{dt}(\theta_{offset} + \delta\theta) = \dot{\delta\theta}$ and $\frac{d^2}{dt^2}(\theta_{offset} + \delta\theta) = \ddot{\delta\theta}$. When $\delta\theta$ converges to 0, equation (15) can be linearized around operating point as:

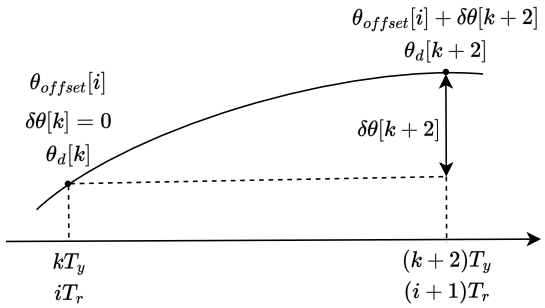

Fig.5 The schematic of the proposed multirate control system

$$T_m = \underbrace{J\delta\ddot{\theta} + D\delta\dot{\theta} + U\cos\theta_{offset}\delta\theta}_{\text{Linear Dynamics}} + \underbrace{U\sin\theta_{offset}\cos\delta\theta}_{\text{Nonlinear Dynamics}} \tag{15}$$

There are both linear dynamics and nonlinear dynamics in (15) and (16). For the nonlinear dynamics, refers to (13) and (14), can be directly feed-forwarded. The nonadaptive state space of the linear part shown in (16) and the nonadaptive MNC can be expressed in (16) where the state variable $\boldsymbol{x} = \begin{bmatrix}\theta_d & \dot{\theta}_d\end{bmatrix}^{\mathrm{T}}$ is shown in (16) and the system input u is the inout torque.

$$\begin{aligned}\dot{\boldsymbol{x}} &= \begin{bmatrix} 0 & 1 \\ -\frac{U\cos\theta_{offset}}{J} & -\frac{D}{J}\end{bmatrix}\boldsymbol{x} + \begin{bmatrix}0 \\ \frac{1}{J}\end{bmatrix}u,\ y = \begin{bmatrix}1 & 0\end{bmatrix}\boldsymbol{x} \\ \boldsymbol{u}_{MNC}[i] &= \begin{bmatrix}U\sin(\theta_{offset}[i]) & U\sin(\theta_{offset}[i])\cos(\delta\theta[k+2])\end{bmatrix}^{\mathrm{T}}\end{aligned} \tag{16}$$

For the adaptive case, the J, D, U can be replaced by $\hat{J}$, $\hat{D}$, $\hat{U}$ from the RLS identification. Then We can easily obtain the multirate state-space matrices of (17) by discretize state-space following discrete law of (9).

The PTC generates the feedforward signal at every T_r samples, and the input desired sate trajectory is $\boldsymbol{x}_d[iT_r]$ and $\boldsymbol{x}_d[(i+1)T_r]$. As illustrated in Fig. 5, we chose the iT_rth sample as the operating point and decompose the system dynamics into θ_{offset} and $\delta\theta$. As we stated in (4), the input desired reference states are $\boldsymbol{x}_d[iT_r] = \begin{bmatrix}\theta_d[k] & \dot{\theta}_d[k]\end{bmatrix}^{\mathrm{T}}$ and $\boldsymbol{x}_d[(i+1)T_r] = \begin{bmatrix}\theta_d[k+2] & \dot{\theta}_d[k+2]\end{bmatrix}^{\mathrm{T}}$. In this proposed method, the state variable $\boldsymbol{x}_d$ are replaced as:

$$\begin{aligned}\boldsymbol{x}_d[iT_r] &= \begin{bmatrix}\theta_d[k] - \theta_{offset} \\ \dot{\theta}_d[k] - 0\end{bmatrix} = \begin{bmatrix}0 \\ \dot{\theta}_d[k]\end{bmatrix} \\ \boldsymbol{x}_d[(i+1)T_r] &= \begin{bmatrix}\theta_d[k+2] - \theta_{offset} \\ \dot{\theta}_d[k+2] - 0\end{bmatrix} = \begin{bmatrix}\delta\theta \\ \dot{\theta}_d[k+2]\end{bmatrix}\end{aligned} \tag{17}$$

Notice that the θ_{offset} and $\delta\theta$ are position-dependent variables that updates at evert sampling time T_r.

4. Simulation Validation

〈4•1〉 Simulation Setup By using Matlab/Simulink and the parameters in Table 2, we established a simulator of the proposed system. No measurement noises and coulomb friction involved in all the simulations. The PID controller in this section is designed by pole placement to the close-loop system including PID and the nominal plant $G(s) = (Js^2 + Ds)^{-1}$, where J and D are the same as the simulation plant. The desired poles of the closed-loop system including the PID controller and the nominal plant are selected at 10π.

The reference trajectory and the PE index are shown in Fig. 6 and they are designed as a periodic S-curve signal move between 0 degree to 90 degree at every second. The PE conditions in this research are shown as:

$$\theta > 0.1 \text{ rad and } |\dot{\theta}| > 0.5 \text{ rad/s and } |\ddot{\theta}| > 1 \text{ rad/s}^2 \tag{18}$$

As we stated in 3.1, the RLS would identify the parameters only when (18) is satisfied.

〈4•2〉 Simulation Results

〈4•2•1〉 Comparison between proposed algorithms This section is to evaluate the control performance of the proposed algorithms in the ideal situation. To this end, the nonadaptive PTCs

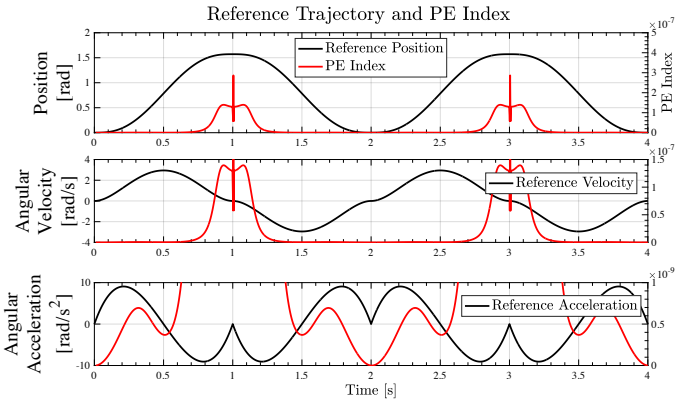

Fig.6 The desired trajectory with pre-calculated PE index ($\kappa > 0$) used in simulations and experiments

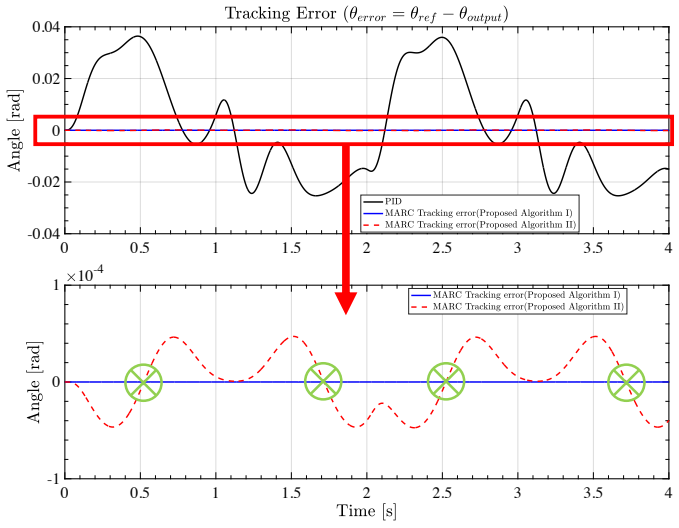

Fig.7 The tracking error comparison of proposed MARC(s) with the system parameter estimations

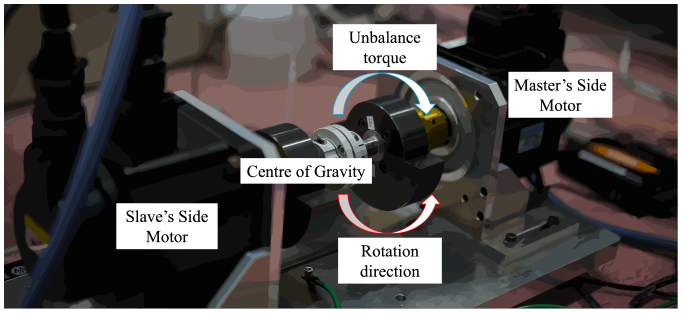

Fig.8 Unbalance torque test bench used in this study.

Table 2 Experiment setup

	J	D	U	Description
Nominal	20e-4	10e-3	10e-2	Non-adaptive
RLS Initial Estimation	20e-4	10e-3	10e-2	Adaptive
λ_{RLS}	0.995	0.950	0.900	Conditional update (18)

Table 3 Tracking performance of the experiments

	PID	Proposed I	Proposed II	Description
RMSD	0.0226	0.0162	0.0160	Nonadaptive (Fig. 9)
		0.0107	0.0106	Adaptive (Fig. 10)

with PID controllers are designed based on the proposed algorithms by using the true parameters of the plant.

The simulation result is shown in Fig. 7, from where we can learn that even the PID controller designed base on the true model can not achieve perfect tracking. The 2 proposed methods in ideal situation can significantly improve the tracking performance where algorithm I is better than algorithm II who has a periodic ahead/behind of the tracking error. The periodic error of algorithm II is due to the fact that the linearized model has a certain level of mismatch with the actual nonlinear model. This causes the performance deterioration, as the algorithm II cannot generate enough feedforward command to track the reference trajectory. The cross points of the tracking error are marked as in Fig. 7.

5. Experimental Validation

〈5•1〉 Experimental Setup The experimental system is shown in Fig. 8. The unbalanced load(s) simulates the tilting table and they are connected by a damping. The loads are powered by 2 motors with same input current command. The motor has the rated power of 1.6 kW, the rated torque of 5.09 Nm, and the peak torque of 15.27 Nm. The control system is implemented in C program and the fundamental sampling rate $T_u = T_y = 4 \times 10^{-4}$s, the sampling rate of the reference signal $T_r = 8 \times 10^{-4}$s and in concern of the computational burden and anti-noise the RLS algorithm can be performed with a longer period $T_{RLS} = 4 \times 10^{-3}$s.

The experimental setup is introduced in Table 2 and for tracking control purpose, the PID controller is designed by pole placement to the close-loop system including PID and the nominal plant $G_n(s) = (J_n s^2 + D_n s)^{-1}$. By a fine tuning process, the poles of the closed-loop system are selected as 10π.

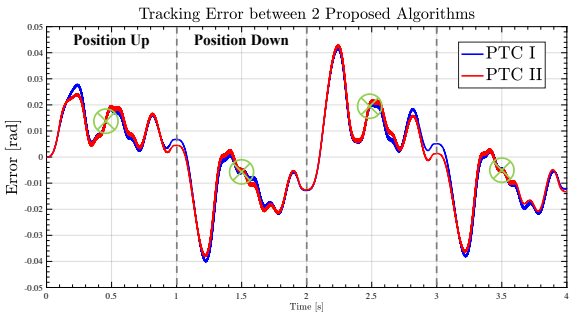

Fig.9 Comparison of tracking errors of two proposed algorithm without parameter updated (non-adaptive)

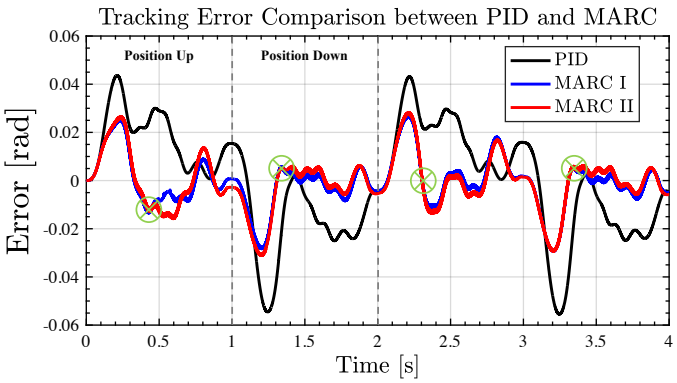

Fig.10 The tracking error of the PID and the MARC(s)

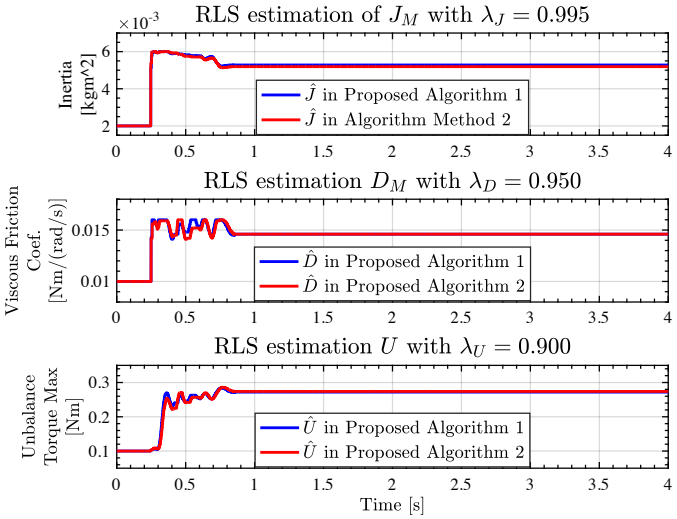

Fig.11 The RLS estimation of the proposed methods

〈5•2〉 Experimental Results

〈5•2•1〉 Comparison of the proposed algorithms This section is to evaluate the control performance of the proposed algo-

rithms in real experimental situation including measurement noises and coulomb friction. The proposed control system was performed without updating the identified parameters from the RLS base on the proposed algorithms respectively with the same PID feedback controller. As we mention in Section 4.2.1, the tracking error of proposed algorithm II is behind of algorithm I in 0 to 0.6s and 1.5 to 2.5s. On the other hand, the tracking error of proposed algorithm II is ahead of algorithm I in 0.6 to 1.5s and 2.5 to 3.5s.

〈5・2・2〉 MARC validation The tracking error of the PID and the proposed algorithms are shown in Fig. 10, with the update conditions shown as (18), the RMSD of the tracking error is shown in Table 4. The tracking performance is improved 52.6% and 53.0% respectively for algorithm I and II evaluated by RMSD. Notice that there are 4 peaks of tracking errors, for example, the tracking error between 1s and 1.5s. This is because of the change of moving directions that leads to a change of coulomb friction. The 2 proposed algorithms can achieve the similar tracking performance despite of the linearization in algorithm II. The RLS estimation result for Section 5.2.2 is given as Fig. 11. Notice that the true dynamics in the test bench contains coulomb friction and such nonlinearity can not be estimated using RLS.

6. Conclusion

In this paper, we presented a basic study on nonlinear estimation and compensation based on RLS algorithm. Two algorithms have been proposed for multi-rate nonlinear compensator, which is integrated to the multi-rate control system including the feedforward and feedback controllers. The effectiveness of the proposal has been verified by both numerical simulation and experiment. The two algorithms achieved the same level of positioning tracking control, and the control performance is significantly improved in comparison with the conventional system consisting of only PID controller. In the future, we will thoroughly examine the proposed method by considering the analysis of the inter-sample control performance. Online estimation and compensation of the friction could be another research interest. Besides, we will investigate the design approach that rigorously guarantee the stability of the system with respect to the nonlinearity.

References

（1） DMG MORI CO.,LTD, ”An Introduction to 5-axis Processing,” https://www.dmgmori.co.jp/sp/5axis/ (Accessed on 24th of July, 2023).

（2） D. Y. Ohm, ”Analysis of PID and PDF compensators for motion control systems,” Proceedings of 1994 IEEE Industry Applications Society Annual Meeting, Denver, CO, USA, Vol.3, No.2 p.1923-1929 (1994).

（3） Deng, C., Xie, S.Q., Wu, J. et al, ”Position error compensation of semi-closed loop servo system using support vector regression and fuzzy PID control,” Int J Adv Manuf Technol, Vol.71, No.5 p.887–898 (2014).

（4） D. G. A. Krishna, K. Anbalagan, K. K. Prabhakaran and S. Kumar, ”An Efficient Pseudo-Derivative-Feedback-Based Voltage Controller for DVR Under Distorted Grid Conditions,” in IEEE Journal of Emerging and Selected Topics in Industrial Electronics, Vol. 2, No. 1, pp. 71-81 (2021).

（5） T. Atsumi, ”Feedforward Control Using Sampled-Data Polynomial for Track Seeking in Hard Disk Drives,” in IEEE Transactions on Industrial Electronics, Vol. 56, No. 5, pp. 1338-1346 (2009).

（6） H. Fujimoto, Y. Hori and A. Kawamura, ”Perfect tracking control based on multirate feedforward control with generalized sampling periods,” in IEEE Transactions on Industrial Electronics, Vol. 48, Vo. 3, pp. 636-644 (2001).

（7） Ohnishi, Wataru, et al. ”State-tracking Iterative Learning Control in Frequency Domain Design for Improved Intersample Behavior,” International Journal of Robust and Nonlinear Control, Vol. 33, No. 7, pp. 4009-4027 (2023).

（8） Horowitz, R., and Tomizuka, M. ”An Adaptive Control Scheme for Mechanical Manipulators—Compensation of Nonlinearity and Decoupling Control.” ASME. J. Dyn. Sys., Meas., Control, Vol. 108, No. 2, pp, 127-135, (1986).

（9） L. Blanken, F. Boeren, D. Bruijnen and T. Oomen, ”Batch-to-Batch Rational Feedforward Control: From Iterative Learning to Identification Approaches, With Application to a Wafer Stage,” in IEEE/ASME Transactions on Mechatronics, Vol. 22, No. 2, pp. 826-837 (2017).

（10） H. Fujimoto and Bin Yao, ”Multirate adaptive robust control for discrete-time non-minimum phase systems and application to linear motors,” in IEEE/ASME Transactions on Mechatronics, Vol. 10, No. 4, pp. 371-377 (2005).

（11） Yao, Bin, and Andrew Palmer. ”Indirect adaptive robust control of SISO nonlinear systems in semi-strict feedback forms.” IFAC Proceedings Volumes, Vol. 35, Vo. 1, pp. 397-402 (2001).

（12） K. Ohno, H. Fujimoto, Y. Isaoka and Y. Terada, ”Adaptive Cutting Force Observer for Machine Tool Considering Stage Parameter Variation,” 2021 IEEE International Conference on Mechatronics (ICM), Kashiwa, Japan, pp. 1-6, (2021).